

Adsorption Performance of Packed Bed Column for the Removal of Lead (II) using Velvet Tamarind (*Dialium indum*) Shells

Abstract

The removal of Pb ions by activated carbons prepared from velvet tamarind (*Dialium indum*) shells was studied to investigate its uptake potentials using Column sorption at different operating conditions (Flow rates, different initial concentrations, bed height). The prepared adsorbent was characterized by determining the physicochemical properties, proximate analysis, CHNS analysis, FT-IR, Potentiometric titration. Different dynamic models were used to describe the sorption processes. The FTIR analysis results suggested the presence of functional groups such as hydroxyl, carbonyl, carboxyl and amine which could bind the metals and remove them from the solution. The values of moisture content, volatile matter, fixed carbon and ash content as obtained from % proximate analysis are 3.43, 27.07, 65.05, 4.45 for activated carbons prepared from velvet tamarind shells. Ultimate analysis revealed that activated carbons prepared from velvet tamarind shells contained 75% carbon. The surface area and Iodine Number of activated carbon from velvet tamarind shell are 570 m²/g and 614.7 mg/g respectively. The column experimental data revealed that an increase in bed height and initial metal concentration or a decrease of flow rate enhances the longevity of column performance by increasing both breakthrough time and exhaustion time thereby delaying bed saturation. Low ash content and high surface areas are indication of good mechanical strength and microporosity of the activated carbons prepared from this precursor. The activated carbons are inexpensive and appeared to be effective and can be explored for future commercial application for environmental sustainability.

Key words: Adsorbent, Velvet tamarind, adsorption, Pollution, Lead

1.0 INTRODUCTION

The geometrical increase in the world population as well as increase in industrial activities has made environmental pollution an important issue of serious concern (Singh *et al.*, 2006). Gaseous, liquid and solid wastes emanate from these activities. Earth's surface is made up of 70% water which is the most valuable natural resource existing on our planet without which life becomes impossible. Although this fact is widely recognized, pollution of water resources is a common problem being faced today. Lakes, rivers and oceans are being overwhelmed with many toxic contaminants (Oliveira *et al.*, 2012). Among toxic substances exceeding threshold levels are heavy metals (Zeng *et al.*, 2004).

Heavy metal pollution occurs directly by effluent discharge from industries such as textiles, dyes, leather tanning, electroplating, metal finishing, refineries, mine water and waste treatment plants and indirectly by the contaminants that enter the water supply from soils/ground water systems and from the atmosphere via rain water. The presence of these toxic substances in an undesirable level in wastewaters makes their removal to receive much attention (Ahluwalia and Goyal, 2005). When heavy metal concentration in waste water is

36 considerably high, it would endanger public health and the environment if discharged into the environment
37 without adequate treatment (Nouri *et al.*, 2006).

38 Several methods such as ion exchange, solvent extraction, reverse osmosis, and precipitation have been used
39 for the removal of heavy metals from aqueous solutions but most of these methods are non-economical and
40 have many disadvantages such as high reagents and energy requirements, generation of toxic sludge of other
41 waste products that also require disposal after treatment (Dermibas, 2008). However, adsorption of heavy
42 metals from aqueous solutions is a relatively new process that has proven very efficient and promising in the
43 removal of contaminants from aqueous effluents where interactions between metal ions and biomass present
44 potential applications for the remediation of metal contaminated waters in various industries (Nouri *et al.*,
45 2006). The process of adsorption has an edge over other methods due to its sludge free clean operation and
46 efficient removal of toxic metals even from dilute solution. It is as an innovative principle of using waste to
47 treat waste and will be more efficient because the agricultural by-products used as adsorbents are readily
48 available, affordable, eco-friendly and have high uptake capacity for heavy metals due to the presence of
49 functional groups which can bind metals to effect their removal from effluents making it more cost effective
50 than the use of commercial activated carbon which is expensive. Alternative activated carbon produced from
51 velvet tamarind fruits will be cheap, locally available and could be used to reduce environmental pollution by
52 heavy metals.

53 The release of toxic metals into the environment would be controlled in this way, and so, the process could
54 be used more extensively as an alternative method to the conventional treatment techniques (Lazaridis *et al.*,
55 2005).

56 Considerable attention has been devoted to the development of unconventional materials like used
57 agricultural by-products for the removal of heavy metals from waste water (Kuma and Jena, 2015), since
58 these plant based by-products represent waste resources, and are widely available and environmentally
59 friendly (Abia and Asuquo, 2007). Various natural adsorbents obtained from agricultural wastes like sun
60 flower stalk, Eucalyptus bark, maize husk, coconut shell, waste tea, rice straw, tree leaves, peanut and walnut
61 husk, palm fruit bunch and African spinach stalk have been tried as raw materials for adsorbents to achieve
62 effective removal of various heavy metals (Sing *et al.*, 2006; Kahraman *et al.*, 2008).

63 Commercial activated carbons have been used for the removal of heavy metals but are imported and
64 expensive. There is a need to look for viable non-conventional low-cost adsorbents as alternative to

65 commercial activated carbon in order to meet the growing demand for cheaper and effective adsorbents.
66 Velvet tamarind is among common fruits produced in Nigeria and large volumes of its non-edible and non
67 useful parts such as the shells constitute environmental problems. These non essential parts of velvet
68 tamarind could be explored for the production of activated carbon.

69 The aim of this study is to prepare, characterize and assess the heavy metal adsorption potentials of activated
70 carbons produced from velvet tamarind.

71 **2.0 Materials and methods**

72 **2.1 Sample Collection and Preparation**

73 The carbonaceous precursor used for preparation of activated carbon is velvet tamarind shells that were
74 obtained as agricultural and forest wastes. Prior to use, samples were washed gently with water to remove mud
75 and other impurities present on the surface and then sundried for one week. The samples shells collected after
76 discarding the fruit pulp, were washed with deionized water, sun dried and then dried in a vacuum oven at 80°C
77 for 24 h, crushed and ground using mortar and pestle. The particles were separated by using a US standard
78 testing sieve (No. 100~No. 200). 100 g of raw material was impregnated with 100 cm³ of concentrated H₂SO₄
79 for 12 hours. The impregnation was carried out at 70 °C in a hot air oven to achieve well penetration of
80 chemical into the interior of the precursor. The sieved samples were placed in a crucible and heated in a muffle
81 furnace for 60 minutes at 500°C. Activated carbons produced were cooled in desiccators and rinsed with
82 deionized water until neutral pH was attained and stocked for subsequent heavy metal removal tests and
83 analysis.

84 **2.2 Sample Characterization**

85 The pH, bulk density, iodine number, specific surface area, chemical composition of the adsorbents,
86 Proximate analysis of the activated carbons were determined using standard test (ASTM, 1996, Ahmedna *et*
87 *al.*, 1997, ASTM D 4607-86, 1986, Al-Quodah and Shawabkah, 2009, ASTM D2867 –96). Ultimate
88 Analysis (CHNS elemental analysis) of the samples were determined by subjecting them to combustion
89 process (furnace at ca. 1000°C) for 30 minutes, where carbon was converted to carbon dioxide; hydrogen to
90 water; nitrogen to nitrogen gas/ oxides of nitrogen and sulphur to sulphur dioxide. The combustion products
91 were swept out of the combustion chamber by inert carrier gas and passed over heated (about 600° C) high
92 purity copper situated at the base of the combustion chamber to remove any oxygen not consumed in the
93 initial combustion and to convert any oxides of nitrogen to nitrogen gas. The gases were then passed through

94 the absorbent traps in order to leave carbon dioxide, water, nitrogen and sulphur dioxide which were
95 separated and detected using GC and thermal conductivity detection.

97 **2.3 Fourier Transform Infrared (FTIR) Spectrometer**

98 FTIR analysis was made using IPRrestige-21, FTIR-84005, SHIMADZU Corporation (Kyoto, Japan).
99 Sample of 0.1 g was mixed with 1 g of KBr, spectroscopy grade (Merk, Darmstadt, Germany), in a mortar.
100 Part of this mix was introduced in a cell connected to a piston of a hydraulic pump giving a compression
101 pressure of 15 kPa / cm². The mix was converted to a solid disc which was placed in an oven at 105°C for 4
102 hours to prevent any interference with any existing water vapor or carbon dioxide molecules. Then it was
103 transferred to the FTIR analyzer and a corresponding spectrum was obtained showing the wave lengths of the
104 different functional groups in the sample which were identified by comparing these values with those in the
105 library.

106 **2.4 Preparation of Pb Solution (Simulated Effluent)**

107 Standard Lead (Pb) stock solution (1000 mg/dm³) were prepared by placing 1.578 g Pb(NO₃)₂ in a
108 volumetric flasks to which 100 cm³ of deionised water was added. The flasks were shaken vigorously to
109 ensure the dissolution of the mixture. The solution was made up to 1000 cm³ mark with deionised water. The
110 working concentrations were prepared from the stock solution by serial dilution. pH adjustment of solutions
111 were made using dilute NaOH and HCl solutions. Deionized water was used to prepare all the solutions. All
112 reagents were of analytical grade.

114 **2.5 Fixed Bed Column Experimental procedure**

115 Fixed bed column studies were carried out using a glass column of 30 mm internal diameter and 400 mm
116 length. The activated carbon having 0.425 mm to 0.600 mm particle size range was used. The activated
117 carbon was packed in the column with a layer of glass wool at the top and bottom. Bed height of 50 mm,
118 100 mm and 150 mm were used. The tank containing the heavy metal solution was placed at a higher
119 elevation so that the metal solution could be introduced into the column by gravitational flow. The flow
120 controller helps to regulate the flow rate. Three flow rates (1, 3 and 5 cm³/min) were used while initial ion
121 concentrations of 50, 100 and 150 mg/dm³ were used. The effluent samples were collected at hourly intervals
122 and analyzed for the residual metal concentration using atomic absorption spectrophotometer.

123 2.6 Dynamic models

124 For the successful design of a column adsorption process, it is important to predict the concentration-time
125 profile or breakthrough curve for effluent parameters. A number of mathematical models have been
126 developed for use in the design of continuous fixed bed sorption columns. In this work, the Bed Depth
127 Service Time (BDST), Thomas and Yoon-Nelson models were used in predicting the behaviour of the
128 breakthrough curve because of their effectiveness. The model's equations are presented in equations 1 to 3:

$$129 \text{BDST} = t = \frac{N_0}{CoF} Z - \frac{1}{KaCo} \ln\left(\frac{Co}{CB}\right) - 1 \quad (1)$$

$$130 \text{Thomas} = \ln\left(\frac{Co}{Ct} - 1\right) = \frac{Kthq_0M}{Q} - KthCot \quad (2)$$

$$131 \text{Yoon-Nelson} = \ln\left(\frac{Ct}{Co-Ct}\right) = Kynt - \tau Kyn \quad (3)$$

132

133 The maximum column capacity, q_{total} (mg) for a bed height of 10.00 cm, initial metal concentration of 50.00
134 mg/dm^3 and flow rates of 1.00, 3.00 and 5.00 cm^3/min was calculated from the area under the breakthrough
135 curves as given by the equation 4 (Ahmad and Hameed, 2010)

136

$$137 q_{\text{total}} = \frac{QA}{1000} = \frac{Q}{1000} \int_{t=0}^{t=\text{total}} Cad dt \quad (4)$$

138

139 where $Cad = Ci - Ce$ (mg l^{-1}), $t = \text{total}$ is the total flow time (min), Q is the flow rate (cm min^{-1}) and A is the
140 area under the breakthrough curve (cm^2).

141

142 The equilibrium uptake (qe_{exp}), i.e. the amount of the metals adsorbed (mg) per unit dry weight of adsorbent
143 (mgg^{-1}) in the column, was calculated from equation 5 (Martin-Lara *et al.*, 2012):

$$144 qe_{\text{exp}} = \frac{q_{\text{total}}}{W} \quad (5)$$

145 where W is the total dry weight of Velvet tamarind shell in the column (g)

146 The total volume treated, V_{eff} (cm^3) was calculated from equation 6 (Futalan *et al.*, 2011)

$$147 V_{\text{eff}} (\text{cm}^3) = Qt_{\text{total}} \quad (6)$$

148 The Mass Transfer Zone (Z_m) is one of the widely used parameters to examine the effects of the column
149 adsorption height. To determine the length of the adsorbent zone in the column, Z_m was calculated from
150 equation (7):

$$151 Z_m(\text{cm}) = Z(t_e - t_b/t_e) \quad (7)$$

152 where, L presents the closed height (cm), t_b is the time (minute) required to reach the breakthrough point or
 153 $C_{eff}/C_o = 0.05$ and t_e is the time (minute) required to reach the exhaustion point or $C_{eff}/C_o = 0.95$ (Apiratikul
 154 and Pavasant, 2008).

155 3.0 RESULTS AND DISCUSSION

156 The Proximate Analysis, Ultimate Analysis and physicochemical properties of activated carbons produced
 157 from velvet tamarind shells are presented in Tables 1.0, 2.0 and 3.0

158 **Table 1.0: Proximate Analysis, of the Activated Carbons Prepared from Velvet Tamarind Shells**

Property	Vt
Moisture	3.43
Volatile Matter	27.07
Fixed carbon	65.05
Ash	4.45

159 Key : Vt = activated carbon from velvet tamarind fruit shells

161 **Table 2.0: Ultimate Analysis of Activated Carbons from Velvet Tamarind Shells in Comparison with**
 162 **other Commercial Activated Carbons**

Element	Vt	Cs
C	75	56.48
H	1.2	2.56
N	1.8	0.61
S	0.8	0.23
O	21.5	40.12

163 Cs = activated carbon from coconut shell (Yusup *et al.*, 2010)

164 **Table 3.0: Physicochemical Properties of Activated carbons prepared from Velvet Tamarind shells.**

Parameter	Vt
Bulk density (g/cm^3)	0.51

Iodine number (mg/g)	614.7
Surface area (m ² /g)	570
Particle density (g/cm ³)	0.72
Porosity (%)	26.4
pH	6.9
Pore Volume	0.13

165

166 3.1 Proximate Analysis of Activated Carbons from Velvet Tamarind Shells

167 According to Alam *et al.* (2008), Ash content is the measurement of the amount of mineral (e.g. Ca, Mg, Si
 168 and Fe) in activated carbon. Ash content obtained in this work was 4.45 for activated carbons prepared from
 169 Velvet Tamarind shells (Table 1.0). The ash content of this carbon is well below the typical ash content
 170 values of 8-12% obtained by Yahaya *et al.* (2011) and 12% obtained by Maheswari *et al.* (2008) but higher
 171 than the 3.58 and 4.89 obtained by Mozammel *et al.* (2010) and Gottipati (2012) for coconut and Bael fruit
 172 shell respectively. Typical ash content of activated carbons is around 5 – 6 % (Pandey *et al.*, 2014). A small
 173 increase in ash content causes a decrease in adsorptive properties of activated carbons by reducing the
 174 mechanical strength of carbon and affects adsorptive capacity. The presence of ash has been shown to inhibit
 175 surface development (Valix *et al.*, 2004).

176

177 The value of 78% and 65.05% fixed carbon were obtained from percentage ultimate and proximate analysis
 178 of activated carbon prepared from Velvet Tamarind fruit shells (Table 1.0 & 2.0). Satyawali (2009) prepared
 179 activated carbon from *Euphorbia antiquorum* and obtained 57.94% fixed carbon. Lopez *et al.* (1995)
 180 reported values ranging from 23.7 to 87.13 within 450 to 950°C. Carbonization leads to carbon atoms
 181 rearrangement into graphitic-like structures and the pyrolytic decomposition of the precursor and non-carbon
 182 species elimination, resulting in a fixed carbonaceous char produced (Kanan and Sundaram, 2001). Also
 183 activating agents act as dehydrating agents and oxidants which also influence the pyrolytic decomposition
 184 and prevent the formation of the tar or ash, hence developing the carbon yield. The combine influence of
 185 activation and carbonization increases carbon yield.

186

187 As reported in Table 3.0, the following; 0.51g/cm³, 614.7mg/g, 570m²/g, 26.4% were obtained as the values
188 of bulk density, iodine number, surface area and porosity for activated carbon prepared from Velvet
189 Tamarind shells. The values of bulk density, surface area, and iodine number were similar to the values
190 obtained by Karthikeyan *et al.* (2008). Vijayaraghavan *et al.* (2006) produced activated carbon from palm
191 kernel shell and obtained yields of bulk density of 0.5048g/cm³, iodine number of 766.99mg/g and
192 669.75m²/g BET surface area. Bulk density is the weight per unit volume of dry carbon in a packed bed and
193 is 80-85% of the apparent density (Mohammed *et al.*, 2016). Higher density provides greater volume activity
194 and normally indicates better quality activated carbon. Alikarami *et al.*(2016) in his comparative adsorption
195 studies for the removal of copper (II) from aqueous solution by different adsorbent obtained bulk density
196 values ranging from 0.32 to 0.62. Bulk density of 0.48g/cm³ was obtained by Satyawali, (2009) and is lower
197 than 0.51 g/cm² obtained for velvet tamarind shells.

198
199 The iodine number value is an indication of surface area of the activated carbon (Amuda *et al.*, 2007).
200 Activated carbons with iodine numbers of about 550mg/g can be attractive for waste water treatment from
201 the user's viewpoint (Deheyn *et al.*, 2005).The iodine number values of 614.7 mg/g was obtained for
202 activated carbon prepared from velvet tamarind fruits shells (Table 3.0). These results were within the range
203 of 608 and 746 mg/g obtained by Castro *et al.* (2008). Analysing the Iodine number of activated carbon
204 prepared from palm-oil shell by pyrolysis and steam activation in a fixed bed reactor, Vijayaraghavan *et al.*
205 (2006) obtained maximum value of 766.99 mg/g at 750°C. According to Al-Quodah and Shawabkah (2009),
206 each 1.0mg of iodine adsorbed is ideally considered to represent 1.0 m² of activated carbon internal area.
207 Therefore the adsorbents have enough internal surface area for adsorption.

208 **3.2 Surface Area of Activated Carbons from Velvet Tamarind and Sandal Fruit Shells**

209 Surface area is the carbon particle area available for adsorption. In general, the larger the effective surface
210 area, the greater is the adsorption capacity. A surface area of the activated carbons used in this study is as
211 reported in Table 4.0. The results indicated that the surface area of 570 m²/g was obtained for velvet tamarind
212 shells activated carbon. The specific surface area as indicated in Table 4.0 further confirmed the porous
213 nature of the activated carbons. According to Liu and Liu (2008), an adsorbent with a surface area of 500
214 m²/g and above has a well formed microporous structures suitable for adsorption. According to Castro *et al.*

215 (2008), 95% of the total surface areas of a given adsorbent are micropores. Yang and Duri (2005) stated that
216 most widely used commercial activated carbon has surface areas of between 600-1000 m²/g.

217 **3.3 pH of Activated Carbons from Velvet Tamarind Fruit Shells**

218 The pH of activated carbon can be defined as the pH of a suspension of carbon in distilled water. The
219 chemical nature of the carbon surfaces are mostly deduced from the acidity or pH of the carbon. Table 4.0
220 presented the pH of the activated carbon prepared from velvet tamarind fruits shells as 6.9. The results
221 suggest weakly acidic surface properties. Similar results were obtained by Alothman *et al.* (2011). Valix *et*
222 *al.* (2004) obtained pH between 6.4 and 7.4 for activated carbon prepared from bagasse.

223 **3.4 Moisture content of activated carbons from Velvet Tamarind Shells**

224 Moisture content was measured from loss of water over initial weight of raw materials. Usually moisture
225 content decreases as the temperature increases. As presented in Table 4.0, moisture content of 3.43% was
226 obtained for the activated carbon prepared from Velvet tamarind fruits shells. Vijayaraghavan *et al.* (2006)
227 obtained values between 8.35 to 11.38% for moisture content while Maheswari *et al.* (2008) obtained 4.33%
228 in their work. The moisture contents of commercial activated carbons ranged between 2- 10 % (Yang and
229 Duri, 2005). The practical limit for the level of moisture content allowed in the activated carbon varies within
230 3 to 6% (Kuma and Jena, 2015). The moisture content of 3.43% obtained for the the activated carbon
231 prepared from Velvet tamarind fruits shells activated carbons therefore fall within the practical limit.

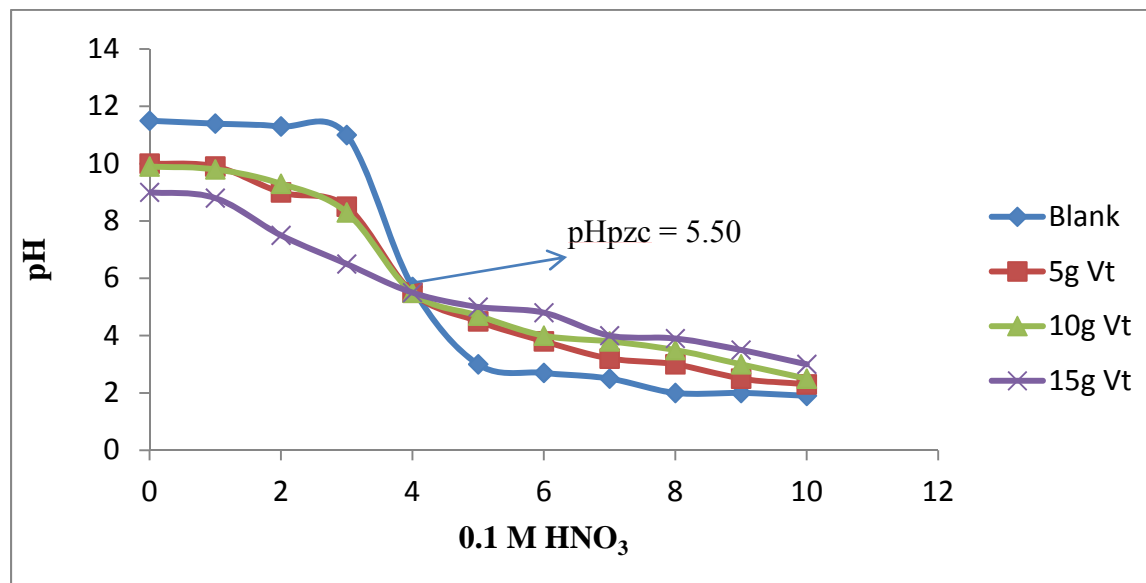
232 **3.5 Volatile matter of activated carbons from velvet tamarind shells**

233 The values of volatile matter of 27.07% (Table 1.0) was obtained for Velvet tamarind fruit shells activated
234 carbons. Lou *et al.* (1999) studied chars prepared from oil palm waste and obtained % volatile matter ranging
235 from 74.86 to 4.08% between 450 to 950°C.

236 **3.6 Potentiometric titration curves of activated carbons from velvet tamarind fruit shells**

237 Figures 1.0 indicate the result of Potentiometric curves of the activated carbons investigated to determine the
238 Point of Zero Charge on the surface of the adsorbent. The point of zero charge (PZC) is an adsorption

239 phenomenon which describes the condition when the electrical charge density on a surface is zero. The
240 common intersection point of the titration curves with the blank is the pH at PZC (pH_{PZC}). From the curves
241 (Figure 1.0), the pH_{PZC} for activated carbon prepared from velvet tamarind shells were identified as 5.50.
242



243

244 **Figure 1.0: Potentiometric Titration Curves of Activated Carbon from Velvet Tamarind Shell**

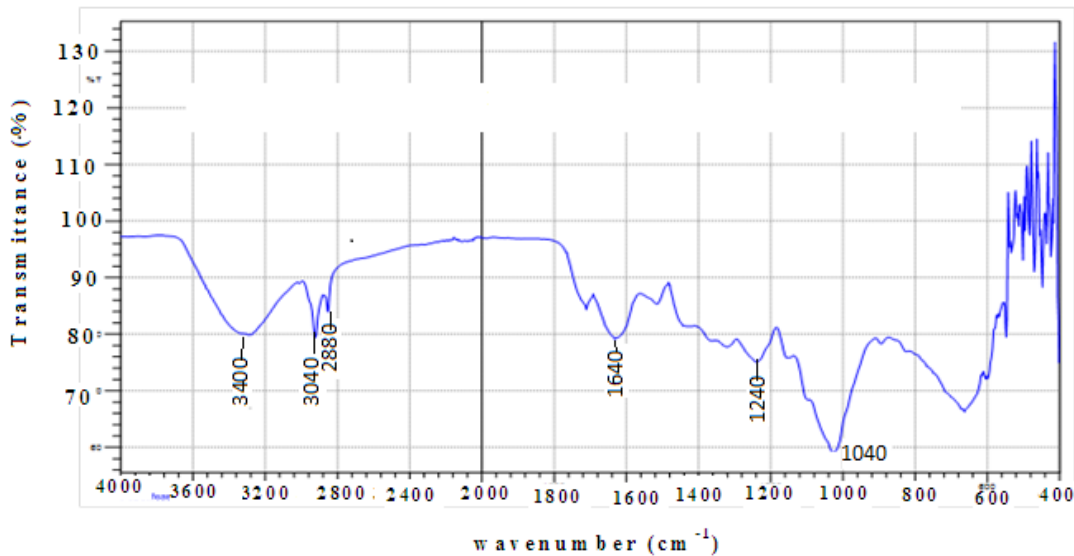
245

246 The titration curve of Velvet tamarind shells is a bit steep. This indicates a moderate capacity of the shells to
247 take up protons (buffering capacity). Therefore, the capacity to take up cationic metals by ionic exchange is
248 probably also moderate. Any pH above $\text{pH}(\text{pzc})$ provide a negatively charged surface favourable for
249 adsorption of cationic heavy metals from the solution.

250 3.7 Fourier transforms infrared spectrometer (FTIR) result of activated carbons from velvet 251 tamarind

252 The FTIR spectral of activated carbons prepared from velvet tamarind fruit shells were used to determine the
253 vibration frequency changes in the functional groups on the surface which facilitates the adsorption of metal
254 ions. The spectra of the activated carbons were measured within the range of $400 - 4000\text{cm}^{-1}$ wave number
255 as shown in Figures 2.0.

256



257

258 **Figure 2.0: FTIR Spectrum of Activated carbon prepared from Velvet Tamarind Shell**

259 The FTIR analysis result (Figure 2.0) suggest the presence of such functional groups as the carboxylic acid
 260 or alcoholic O-H bond stretching which may overlap with amine (N-H) bond stretching at peaks between
 261 3250-3400 cm^{-1} ; possible C=O bond of carbonyl or amide groups within 1640-1670 cm^{-1} ; C-O and O-H bond
 262 stretching of alcohol and ethers at 1000-1260 cm^{-1} of the finger-print region (Gimba et al, 2001). The
 263 important parameters that influence and determine the adsorption of metal ions from aqueous solutions are
 264 the carbon-oxygen functional groups present on the carbon surface and the pH of the solution (Bansal and
 265 Goyal, 2005).

266

267 **3.8 Column Adsorption Studies of Lead (Pb) on Activated carbon Prepared from Velvet Tamarind** 268 **Shells**

269 **3.8.1 Effect of bed height**

270 The adsorption of metal ions in the packed bed column is largely dependent on the bed height, which is
 271 directly proportional to the quantity of adsorbent in the column. The effect of bed height on breakthrough
 272 curve analysis was studied by varying the bed height from 5 cm to 15 cm at increment of 5cm. The
 273 adsorption breakthrough curves were obtained by varying the bed heights at a flow rate of $1\text{cm}^3/\text{min}$ and an
 274 inlet Pb ions concentration of $50\text{mg}/\text{dm}^3$. The breakthrough curves are presented in Figures 2.0. Faster
 275 breakthrough curves were observed for a bed height of 5 cm compared to the bed height of 10 cm and 15 cm.

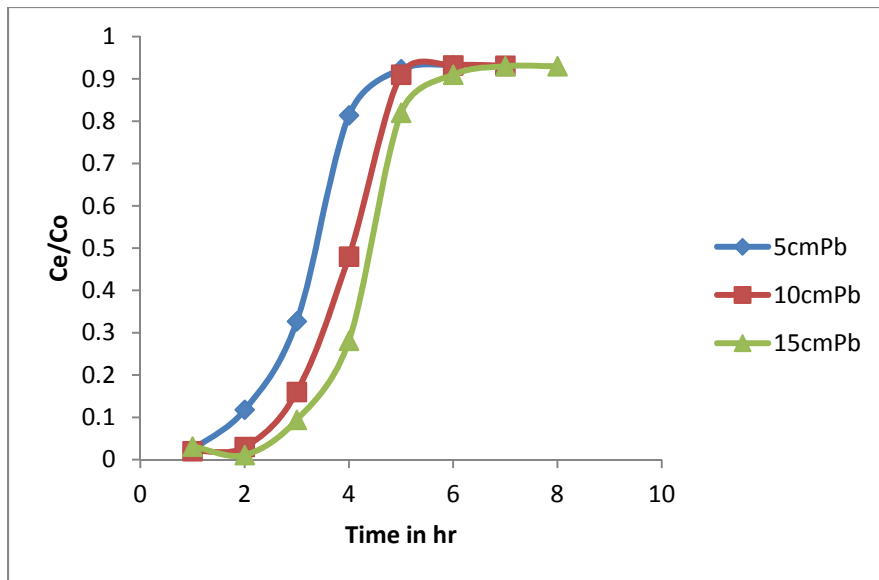


Figure 3.0: Column adsorption of Pb(II) by Activated Carbon from Velvet Tamarind Fruits Shells at different Bed height

As depicted by Figure 3.0, the breakthrough time varied with bed height. Steeper breakthrough curves were achieved with a decrease in bed depth. The breakthrough time decreased with a decreasing bed depth from 15 to 5 cm, as binding sites were restricted at low bed depths. At low bed depth, the metal ions do not have enough time to diffuse into the surface of the adsorbents, and a reduction in breakthrough time occurs. Conversely, with an increase in bed depth, the residence time of metal ions solution inside the column was increased, allowing the metal ions to diffuse deeper into the adsorbents.

The results indicate that the throughput volume of the aqueous solution increased with increase in bed height, due to the availability of more number of sorption sites (Satyawali, 2009). At higher bed depth of 10 cm, adsorbent mass was more residing in the column thereby providing larger service area for binding, fixation, diffusion and permeation of the solute to the adsorbent. Longer bed depth also provided more reaction area and larger volume of influent treatment which translated to higher adsorption capacity.

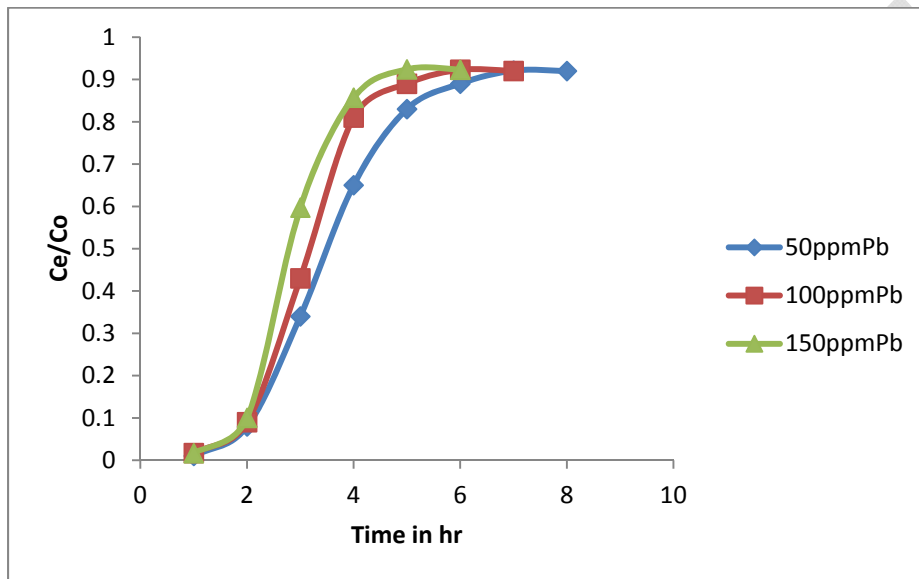
The equilibrium sorption capacity decreased with increase in bed height. This shows that at smaller bed height, the effluent adsorbate concentration ratio increased more rapidly than for a higher bed height. Furthermore, the bed is saturated in less time for smaller bed heights. The slope of the S-shape from t_b to t_e decreased as the bed height increased from 5 to 15 cm, indicating the breakthrough curve becomes steeper as

297 the bed height decreased. Also the breakthrough time (t_b) and exhaustion time (t_e) increase with increase in
298 bed depth

299 3.8.2 Effect of Initial Metal Concentration

300 A Series of column experiments with different metals concentrations namely, 50, 100 and 150 ppm were
301 conducted to investigate the effect of initial metal concentration on the performance of the fixed-bed
302 operation. Figure 3.0 presented the breakthrough curves for the adsorption of Pb onto Velvet tamarind fruit
303 shells activated carbon at various initial metal concentrations.

304 .



305

306 **Figure 4.0: Column adsorption of Pb(II) by Activated Carbon from Velvet Tamarind Fruit shells at**
307 **different Initial Concentration.**

308 .

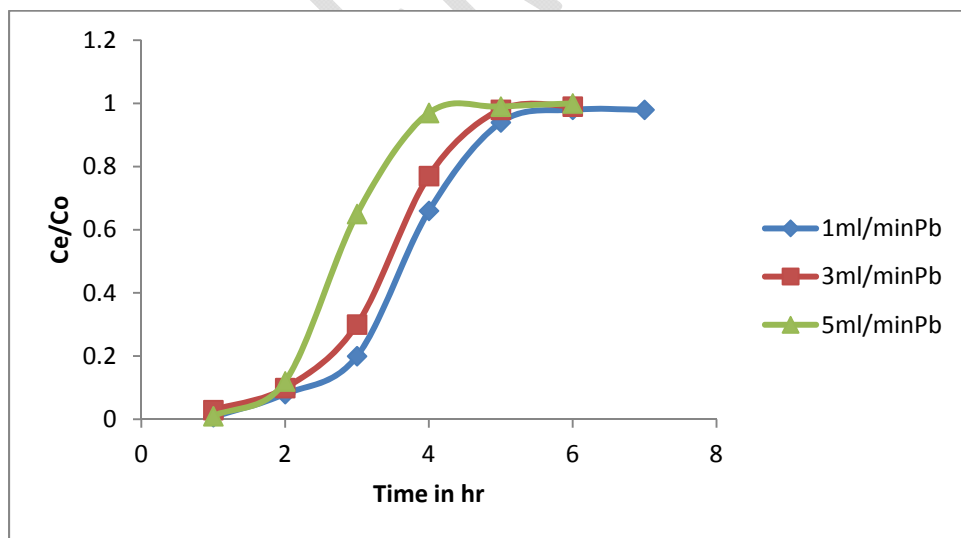
309 It can be seen from the Figure 4.0 that breakthrough curves display three important features: an initial lag
310 period during which effluent metal ions are non-detectable, followed by a rise in concentration, and finally a
311 period of slow increase in effluent level. It was assumed that the breakthrough metal-concentration would be
312 5% of the influent concentration. It is evident that by increasing initial metal concentration, the slope of the
313 breakthrough curve increased and became much steeper, hence reducing the volume which can be treated
314 before breakthrough occurred. This is due to the fact that by increasing the initial metal concentration, the
315 driving forces increases which enhance the rate of metal adsorption and saturates the binding sites more
316 quickly. This is consistent with results of the finding of Betzy and Soney (2015), where the authors found

317 that by increasing inlet adsorbate concentration, the slope of the breakthrough curve increased and the
318 volume treated before carbon regeneration reduced. This behaviour was attributed to the high concentrations
319 which saturated the activated carbon more quickly, thereby decreasing the breakthrough time. It is also clear
320 from Figures 1.0 to 5.0 that all the curves exhibit a characteristic “S” shape which indicates an effective use
321 of adsorbent (Tamura, 2003)

322 3.8.3 Effect of flow rate on breakthrough curves

323 The adsorption columns were operated with different flow rates (1, 3 and 5 cm³/min) until no further metal
324 ions removal was observed. The adsorbent bed height and inlet initial metal ions concentration were fixed at
325 10 cm and 50 mg/dm³, respectively. The breakthrough curve for a column was determined by plotting the
326 ratio of the C_e/C_0 (C_e and C_0 are the metal ions concentration of effluent and influent, respectively) against
327 time, as shown in Figures 1.0 to 5.0 respectively. The effect of the flow rate on the adsorption of Cu, Cd, Pb
328 and Ni are shown as breakthrough curves in the figures. It was observed that breakthrough generally
329 occurred faster with higher flow rate. The reason is that at higher flow rate, the rate of mass transfer
330 increased, thus the amount of metal ions adsorbed onto the unit bed height (mass transfer zone) increased
331 (Patil *et al.*, 2006). In addition, the adsorption capacity decreases with increase in flow rates due to
332 insufficient residence time of the solute in the column and lack of diffusion of the solute into the pores of the
333 adsorbent, therefore the solute left the column before equilibrium occurred. These results were in agreement
334 with other findings as reported by Volesky (2005).

335



336

337 **Figure 5.0: Column adsorption of Pb(II) by Activated Carbon from Velvet Tamarind Fruits Shell**
338 **Activated Carbon at different Flow rate.**

339

340 The column performed well at the lowest flow rate (1cm³/min). Earlier breakthrough and exhaustion times
341 were achieved, when the flow rate was increased from 1 to 5 cm³/min. This was due to a decrease in the
342 residence time, which restricted the contact of metal ions to the adsorbents. Similar results have been found
343 for As (III) removal in a fixed-bed system using modified calcined bauxite and for color removal in a fixed-
344 bed column system using surfactant-modified zeolite (Hrapovic and Rowe, 2002).

345 **3.9 Column Kinetic Study**

346 Three models (Thomas model, Yoon-Nelson and BDST models) were used to analyze the column
347 performance.

348

349 **3.9.1 Thomas model**

350 The model was applied to the experimental data with respect to the initial metals concentration, flow rate and
351 bed height. The kinetic coefficient, kTh and the adsorption capacity of the bed, q₀ were determined from the
352 plot of $\ln\left(\frac{C_0}{C_e} - 1\right)$ against t The results of kTh, R² and q₀ are given in Table 4.0. The results showed that the
353 kinetic coefficient kTh is dependent on flow rate, initial ion concentration and bed height. The maximum
354 adsorption capacity q₀ and Kinetic coefficient kTh decreased with increase in flow rate but increased with
355 increase in bed height and initial ion concentration. The values of kTh obtained in this work is similar to the
356 ones obtained by Yaya (2011). High values of regression coefficients were obtained indicating that the
357 kinetic data conformed well to Thomas model in contrast with the report of Sasikala and Muthuraman (2016)
358 but in agreement with the results obtained by Baek *et al.* (2007). The trend observed with the calculated
359 values of kTh, q₀ are in agreement.

360 **3.9.2 Yoon and Nelson Model**

361 This model is based on the assumption that the rate of decrease in the probability of adsorption for each
362 adsorbate molecule is proportional to the probability of adsorbate adsorption and the probability of adsorbate
363 breakthrough on the adsorbent (Kavak and Öztürk, 2004). The Yoon and Nelson equation for single
364 component system is expressed as shown in equation 4.3 (Aksu *et al*, 2004):

$$365 \quad \ln \frac{C_e}{C_0 - C_e} = K_{yn}t - \tau K \quad (4.3)$$

366 Yoon and Nelson model has been used in the study of column adsorption kinetics (Kavak and Öztürk, 2004,
367 Satyawali, 2009). The values of the Yoon-Nelson parameters (k_{yn} and τ) were determined from the plot of
368 $\ln \frac{C_e}{C_0 - C_e}$ versus t at various operating conditions (Table 1.0 to 5.0). A plot of $\ln \frac{C_e}{C_0 - C_e}$ versus t gives a
369 straight line with slope of K_{yn} , and intercept of $-\tau K$. The results showed that the rate constant, K_{yn} increased
370 with increased inlet ions concentration, flow rate and bed height. The time required for 50% breakthrough, τ
371 decreased with increase in flow rate and initial ion concentration. High values of correlation coefficients
372 obtained indicate that Yoon and Nelson model fitted well to the experimental data and can be used to
373 describe the Cd(II), Cu(II), Pb(II) and Ni(II)-Velvet Tamarind shell and Cd(II), Cu(II), Pb(II) and Ni(II) –
374 Sandal fruit shell biosorption system.

375

376

377

378

UNDER PEER REVIEW

380 **Table 4.0: Column kinetic parameters for Pb ions adsorption on activated carbon from Velvet tamarind fruit Shells**

	Initial ion concentration(mg/dm ³)			Flow rates in cm ³ /min			Bed height (cm)		
	50	100	150	1	3	5	5	10	15
Thomas K _{Th} (cm ³ /min/mg) X10 ⁻³	2.40	7.20	2.30	0.34	0.38	0.64	0.24	0.42	0.42
q _o (mg/g)	1.20	1.93	2.80	0.71	0.38	2.10	1.00	1.20	1.80
R ²	0.98	0.97	0.95	0.98	0.99	0.98	0.96	0.95	0.99
Yoon & Nelson K _{yn} (min ⁻¹) X10 ⁻²	1.00	1.40	2.00	1.60	2.00	2.50	1.90	1.90	3.10
τ (min)	251.00	205.00	125.00	173.00	167.00	126.00	125.00	150.00	194.00
R ²	0.95	0.99	0.94	0.97	0.99	0.94	0.97	0.99	0.97

382 3.9.3 Lead Uptake in the Column at Different Operating Parameters

383 This study showed that the sorption uptake capacity of the column Pb 1.73 mg g⁻¹ for velvet tamarind
384 fruit shells activated carbon as shown in Table 5.0. The increased capacity of the column method is
385 largely due to the continuous increased concentration gradient in the interface of the adsorption zone
386 as it passes through the column, whereas the gradient concentration decreases with time in batch
387 systems (Sousa, 2010; Martin-Lara *et al.*, 2012).

388

389 A characterisation study on the Velvet Tamarind shells prior to biosorption showed that hydroxyl and
390 carboxylic functional groups were present and might be involved in the removal of metal ions from
391 aqueous solutions by this biosorbent, besides micro precipitation and electrostatic attraction forces.
392 The results obtained by Sousa (2010) for Ni(II), Cd(II), Zn(II) and Pb(II) ions using H₂SO₄ treated
393 coconut shell suggest that a lower pH of 6 is required for optimal removal of the studied metals,
394 similar to the pH of 6 ± 0.2 used in this study.

395 **Table 5.0: Uptake of Pb(II) by activated carbon from Velvet Tamarind Fruit shells at different**
396 **flow rates**

	Z	Q	C ₀	V _{eff}	q _{total}	q _{e(exp)}	Z _m
	(cm)	(cm ³ min ⁻¹)	(mg dm ⁻³)	(cm ³)	(mg)	(mgg ⁻¹)	(cm)
Vt	10.00	1.00	50.00	1191.00	1.79	1.73	6.40
	10.00	3.00	50.00	882.00	0.44	1.64	7.95
	10.00	5.00	50.00	300.00	0.30	0.54	5.50

397

398

399 4.0 Conclusion

- 400 i. The experimental data revealed that an increase in bed height and initial metal concentration
401 or a decrease of flow rate enhances the longevity of column performance by increasing both
402 breakthrough time and exhaustion time thereby delaying bed saturation.

- 403 ii. The design of a continuous fixed bed column for removal of metal ions by velvet tamarind
404 and sandal fruit shells activated carbons can be achieved using the BDST, Yoon-Nelson and
405 Thomas models.
- 406 iii. The FTIR analysis results suggested the presence of functional groups such as hydroxyl,
407 carbonyl, carboxyl and amine which could bind the metals and remove them from the
408 solution.
- 409 iv. The values of moisture content, volatile matter, fixed carbon and ash content as obtained
410 from % proximate analysis are 3.43, 27.07, 65.05, 4.45 for activated carbons prepared from
411 velvet tamarind shells.
- 412 v. Ultimate analysis revealed that activated carbons prepared from velvet tamarind shells
413 contained 75% carbon.
414

415

5.0 REFERENCES

- 416 Sing, K. S. W., Everett, D. H., Haul, R. A. W., Moscou, L., Pierotti, R. A., Rouquerol, J., &
417 Siemieniewska, T. (2006). Reporting Physisorption data for gas/solid interface with special
418 reference to the determination of surface area and porosity. *Pure and Applied Chemistry*. 57,
419 603-619.
- 420 Oliveira, R. C., Guibal, E. & Garcia, O. (2012). Biosorption and desorption of lanthanum (III) and
421 neodymium(III) in fixed-bed columns with *Sargassum* sp. Perspectives for separation of rare
422 earth metals. *Biotechnology Progress*, 28(3), 715-722.
- 423 Zeng, L. X., Liand, J., & Liu, X. (2004). Adsorptive removal of phosphate from aqueous solutions
424 using iron oxide tailings. *Water Resources*, 38, 1318-1326.
- 425 Ahluwalia, S. S., & Goyal, D. (2005). Removal of heavy metals by waste tea leaves from aqueous
426 solution. *Engineering and Life Science*, 5(9), 158- 162.
- 427 Nouri, J., Mahvi, A. H., Babaei, A. A., Jahed, G. R., & Ahmadpour, E. (2006). Investigation of heavy
428 metals in groundwater *Pakistan Journal of Biological Science*, 9 (3), 377-384
- 429 Dermibas, A. (2008). Heavy metal adsorption onto agro-based waste materials: A review. *Journal of*
430 *Hazardous Material*, 157(8), 220-229
- 431 Lazaridis, N. K., Matis, K. A., & Diels, L. (2005). 'Application of flotation to the solid/liquid
432 separation of *Ralstonia metallidurans*', *3rd Eur. Bioremediation Conf.*, TU Crete, Chania, 4-7
433 July.
- 434 Abia, A. A., & Asuquo, E. D. (2007). Kinetics of Cd²⁺ and Cr³⁺ Sorption from aqueous solution using
435 mercaptoacetic acid modified and unmodified oil palm fruit fibre (*elaeis*
- 436 Sing, K. S. W., Everett, D. H., Haul, R. A. W., Moscou, L., Pierotti, R. A., Rouquerol, J., &
437 Siemieniewska, T. (2006). Reporting Physisorption data for gas/solid interface with special
438 reference to the determination of surface area and porosity. *Pure and Applied Chemistry*. 57,
439 603-619.
- 440 Kahraman, S., Dogan, N., & Erdemoglu, S. (2008). Use of various agricultural wastes for the removal
441 of heavy metal ions. *International Journal of Environmental Pollution*, 34, 275-284.
- 442 American Society for Testing and Materials. (1986). Standard test method for determination of iodine
443 number of activated carbon. Philadelphia, PA: ASTM Committee on Standards.
- 444 American Society for Testing and Materials. (1996). Standard, Refractories, Carbon and Graphitic
445 Products; activated Carbon, ASTM, Philadelphia, PA, 15(01)
- 446 American Society of Testing and Materials. (1991). Standard test methods for moisture in activated
447 carbon. Philadelphia, PA: ASTM Committee on Standards.
- 448 Ahmedna, M., Johns, M. M., Clarke, S. J., Marshall, W. E., & Rao, R. M. (1997). Potential of
449 agricultural by-product-based activated carbons for use in raw sugar decolourisation. *Journal of*
450 *the Science of Food and Agriculture*, 7(5), 117-124.

- 451 Al-Quodah, Z., & Shawabkah, R. (2009). Production and characterization of granular activated carbon
452 from activated sludge. *Brazilian Journal of Chemical Engineering*, 26(1), 6-10.
- 453 Ahmad, A.A., & Hameed, B.H (2010). Fixed-bed adsorption of reactive azo dye onto
454 granularactivated carbon prepared from waste. *Journal of Hazardous Materials*, 175(1-3): 298-
455 303.
- 456 Apiratikul, R., & Pavasant, P. (2008). Batch and column studies of biosorption of heavy metals by
457 *Caulerpa lentillifera*. *Bioresource Technology*, 99(12), 2766-2777.
- 458 Alam, C., Molina-Sabio, M., & Rodriguez-Reinoso, F. (2008). Adsorption of methane into ZnCl₂-
459 activated carbon derived discs. *Microporous and Mesoporous Materials*, 76(15), 185-191
- 460 Yahaya, N. K. E. M., Abustana, I., Latiff, M. F. I. P. M., Bello, O. S. & Ahmad, M. A. (2011). Fixed-
461 bed column study for Cu (II) removal from aqueous solutions using rice husk based activated
462 carbon. *International Journal of Engineering & Technology*, 11(1), 248-252.
- 463 Maheswari, B. L., Mizon, K. J., Palmer, J. M., Korsch, M. J., Taylor, A.J., & Mahaffey, K.R. (2008).
464 Blood lead changes during pregnancy and postpartum with calcium supplementation.
465 *Environmental Health Perspectives*, 112(15), 1499-1507.
- 466 Yang, X., & Duri, B. A. (2005). “Kinetic modeling of liquid-phase adsorption of reactive dyes on
467 activated carbon”. *Journal of Colloid Interface Sciences*, 287, 25-34.
- 468 Kuma, A., & Jena, H.M (2015) *Applied Surface Science* 356: 753–761.
469
- 470 Lou, M, Garray, R., & Alda, J. (1999). Cadmium uptake through the anion exchange in human red
471 blood cells. *Journal of Physiology*. 443, 123-136.
- 472 Satyawali, Y., & Balakrishnan, M. (2009). Wastewater treatment in molasses-based alcohol distilleries
473 for COD and color removal: A review. *Journal of Environmental Management*, 86, 481-497.
474
- 475 Betzy, N. T., & Soney., C.(2015). Cyanide in industrial wastewaters and its removal: A review on
476 biotreatment. *Journal of Hazardous Materials*, 163, 1-11
- 477 Tamura, H., Hamaguchi, T., & Tokura, S. (2003). “Destruction of rigid crystalline structure to prepare
478 chitin solution”, *Advances in chitin science*. 7, 84–87.
- 479 Patil, S., Bhole, A., & Natrajan, G. (2006). Scavenging of Ni(II) Metal Ions by Adsorption on PAC and
480 Babhul Bark. *Journal of Environmental Science and Engineering*, 48(3), 203-208.
- 481 Volesky, B. (2005). Advances in biosorption of metals: selection of biomass types. *Microbiology*
482 *Reviews*, 14, 291–302.
- 483 Hrapovic, L., & Rowe, R. K. (2002). Intrinsic degradation of volatile fatty acids in laboratory-
484 compacted clayey soil. *Journal of Contaminant Hydrology*, 58, 221- 242
- 485 Sasikala, S., & Muthuraman, G. (2016) Removal of Heavy Metals from Wastewater Using *Tribulus*
486 *terrestris* Herbal Plants Powder. *Iranica Journal of Energy and Environment*, 7(1),39-47.

- 487 Baek, K., Song, S., Kang, S., Rhee, Y., Lee, C., Lee, B., Hudson, S., & Hwang, T. (2007). Adsorption
488 kinetics of boron by anion exchange resin in packed column bed. *Journal of Industrial*
489 *Engineering Chemistry*, 13(3), 452-456.
- 490 Kavak, D., & Öztürk, N. (2004). Adsorption of boron from aqueous solution by sepiolite: II. Column
491 studies. II. Illustrations. *Journal of American Chemical Society*, 23(25), 495-500.
- 492 Aksu, Z., Gönen, F., & Demircan Z. (2004). Biosorption of chromium (VI) ions by Mowital®B30H
493 resin immobilized activated sludge in a packed bed: comparison with granular activated carbon.
494 *Process Biochemistry*, 38(2), 175-186
- 495 Sousa, F. W. (2010). Green coconut shells applied as adsorbent for removal of toxic metal ions using
496 fixed-bed column technology. *Journal of Environmental Management*, 91(8), 1634-1640
- 497 Martín-Lara, M. A., Blázquez, G., Ronda, A., Rodríguez, I.L., & Calero, M. (2012). Multiple
498 biosorption–desorption cycles in a fixed-bed column for Pb(II) removal by acid-treated olive
499 stone. *Journal of Industrial and Engineering Chemistry*, 18(3), 1006-1012
- 500 Gimba, C.E., Olayemi, J.Y., Ifijeh, D.O.H., & Kagbu, J.A. (2001). Adsorption of dyes by powdered
501 and granulated activated carbon from coconut shells. *Journal of Chemical Society of Nigeria*,
502 26(1), 23 -27
- 503 Bansal, M., & Goyal, F. (2005). Removal of Cr(VI) from aqueous solutions using pre consumer
504 processing agricultural waste: A case study of rice husk. *Journal of Hazardous Materials*,
505 162(8), 312–320.
- 506